Heritage Science

RESEARCH ARTICLE

Use of standard analytical tools to detect small amounts of smalt in the presence of ultramarine as observed in 15th-century Venetian illuminated manuscripts

Paola Ricciardi[1†], Kathryn A. Dooley[2†], Douglas MacLennan[3], Giulia Bertolotti[1,4], Francesca Gabrieli[2,5], Catherine Schmidt Patterson[3] and John K. Delaney[2*]

Abstract

A previous preliminary study of 15th-century Venetian manuscript fragments by the Master of the Murano Gradual identified the presence of cobalt in many ultramarine blue areas, suggesting the presence of smalt. This would represent an early use of this glassy pigment in Venetian illuminated manuscripts. Whereas sampling has been used to identify smalt in 15th century paintings, only non-invasive methods can be used on manuscripts due to their small size and fragile nature. Here we investigated four non-invasive analysis techniques to identify small amounts of smalt in the presence of ultramarine, including single-point and scanning XRF spectroscopy, UV–vis-NIR-SWIR reflectance spectroscopy (FORS), Raman spectroscopy, and external reflection FT-IR spectroscopy. This was done by studying paint mock-ups of ultramarine and smalt mixtures with and without the presence of a white pigment on parchment. The results showed molecular spectroscopy techniques (reflectance, Raman, and FTIR) require at least ~30–40% smalt by percent mass when in the presence of ultramarine in order to detect its presence, whereas elemental XRF spectroscopy can detect cobalt (and thus infer the presence of smalt) at the ~1% level. To further explore the inference of smalt by XRF, additional XRF analysis was conducted to specifically look for elements associated with cobalt minerals (i.e. nickel, arsenic, bismuth, etc.). High spatial resolution XRF scanning (60–100 µm X-ray spot size) was used to look for cobalt in smalt particles which are typically larger than those of ultramarine. These two XRF analysis approaches worked well with the mock-up paint samples, and were subsequently applied to the manuscripts for which molecular spectroscopy methods yielded no unambiguous evidence for smalt. The data underscore the challenges of conclusively identifying smalt in complex paint systems when samples are not available, but do suggest that the Master of the Murano illuminated manuscript fragments contain smalt, but perhaps not in a form or amount researchers are used to seeing in paintings.

Keywords: Non-invasive pigment analysis, Smalt, Ultramarine, Master of the Murano Gradual, Venice, Illuminated manuscripts, XRF, Reflectance spectroscopy, Raman, FT-IR

Introduction

The non-invasive identification of artists' pigments can allow significant insights into creative processes and provide information about the often-complex history of a work of art. An artist's choice of a specific pigment can be linked to their artistic vision, a patron's status, the artist's geographic origin, or even historic events (e.g. war

*Correspondence: j-delaney@nga.gov
†Paola Ricciardi and Kathryn A. Dooley contributed equally
[2] National Gallery of Art, 6th Street and Constitution Avenue NW, Washington, DC 20565, USA
Full list of author information is available at the end of the article

Ricciardi *et al. Heritage Science*   (2022) 10:38

Page 2 of 18

disrupting established trade routes). In 15th- and 16th-century Venice only a few blue pigments were available to artists. Most of these were exotic imports to Italy: azurite was imported from Saxony, traversing the Alps [1], whereas natural ultramarine (a sulfur-containing sodium aluminosilicate ($Na_8[Al_6Si_6O_{24}]S_n$)), and indigo reached Venice via the Silk Road from Afghanistan and India, respectively [2, 3]. In contrast, a blue cobalt-containing potassium glass pigment, known as smalt, was locally available as a by-product of the thriving glass industry on the nearby island of Murano and could be obtained at relatively low cost to Venetian artists depending on quality; by the late sixteenth century smalt prices in Venice were similar to those of azurite and indigo, and up to ~350 times lower than ultramarine [4].

Cobalt has been used since antiquity to make blue-colored glass. There is no qualitative difference in chemical composition between cobalt glass and the painters' pigment smalt. As Berrie describes, glass requires less than 2% cobalt to take on a blue color, but painters' pigments would generally require more cobalt (as much as 20%) as the intensity of the color is lost during grinding [5]. Smalt has a much lower tinting strength than ultramarine, and thus smalt pigment particles are typically much larger.

The use of smalt as a pigment in European easel paintings became common in Venice when Titian began to utilize it in the mid-sixteenth century [5, 6] and the pigment appears to have become integral to the palettes of later Venetian masters including Tintoretto and Veronese [7, 8]. In addition to smalt, other glass-based pigments were introduced and slowly integrated into the palette of numerous painters across Europe during the 15th and the 16th century [9, 10]. Outside of Europe, smalt has been found much earlier in wall paintings and illuminated manuscripts [11]. Smalt has been identified with microscopic examination in a wall painting dated to the 11th–12th centuries from Kara Khoto in Inner Mongolia and in wall paintings from the 14th–15th centuries in the monastery of Chora, Constantinople [12]. Smalt has also been identified in Byzantine and Armenian illuminated manuscripts dating from the 13th century based on characteristic absorption bands in visible reflectance spectra and the detection of cobalt from XRF spectra [13].

Only a few examples of the use of smalt in Europe have been found in 15th century paintings [12, 14, 15]. For example, smalt was confirmed in the Dieric Bouts painting *The Entombment*, dated probably to the 1450s, where it was mixed with ultramarine and azurite. Smalt was identified based on microscopic examination of a dispersed pigment sample as well as visible transmittance spectroscopy of the individual particles [12, 14]. Stege used XRF spectroscopy (spot size 80–100 μm) to detect the presence of cobalt in several paintings but was not always able to confirm its presence with light microscopy [15]. In some of these examples, the low cobalt signal in the presence of high copper was interpreted to indicate that the cobalt was likely from an impurity in the copper mineral pigment rather than from smalt. A combination of techniques such as light microscopy (to examine particle morphology), visible transmittance spectroscopy on single particles (to identify electronic transitions), and XRF (through the detection of cobalt) have been selectively used to identify or infer the presence of smalt in 15th century paintings.

Research undertaken for an exhibition at the Fitzwilliam Museum in 2016 examined the pigments used in a manuscript fragment, *Dormition of the Virgin* (Fig. 1a), illuminated by the 15th-century Venetian artist known as the Master of the Murano Gradual (active c. 1420–1450 and also known simply as the 'Murano Master') [16, 17]. This artist, whose identity is unknown, has been named after one in a set of choir books made for the Camaldolese house of San Mattia in Murano and currently held in the Kupferstichkabinett in Berlin. Only one other volume in the set, illuminated by Cristoforo Cortese, survives intact. The other books are now represented by fragments—pages removed from the volumes of a large choir book (called a gradual) two centuries or more ago—dispersed in museums and libraries across the world.

The *Dormition of the Virgin* was analyzed using point-based X-ray fluorescence (XRF) spectroscopy and UV–vis-NIR-SWIR reflectance spectroscopy (FORS). Analysis of the FORS and XRF data collected found the presence of ultramarine in all the blue areas. Interestingly, in some of the blue areas, XRF detected the presence of cobalt, suggesting the possible presence of the pigment smalt [16, 17].

Preliminary analysis of five additional fragments attributed to the same artist (Fig. 1b–f) indicated the presence of cobalt in each. The documenting of the presence of smalt in works by the Murano Master represents among the earliest use of this pigment in European manuscript illumination [18, 19], and therefore also one of the earliest in Western painting [15]. In this paper, a more thorough analysis of the data collected on the Master of the Murano Gradual fragments are presented and discussed in the context of better understanding the ability of the analytical methods used to detect the presence of smalt. As noted above, prior studies identifying smalt in paintings often relied on taking paint samples for microscopic examination; indeed sampling is described in a recent review as being required for the identification of smalt when it is present in mixtures or in complex stratigraphies [11]. This study, however, focuses on illuminated manuscripts, a class of objects for which sampling is

Fig. 1 Illuminated manuscript fragments analyzed, all attributed to the Master of the Murano Gradual. **a** Fitzwilliam Museum, *Dormition of the Virgin*, Marlay cutting It. 18, 30.5 × 32 cm, the illumination that prompted this examination; **b** The J. Paul Getty Museum, *Saint Jerome Extracting a Thorn from a Lion's Paw*, Ms. 106 (2010.21) recto, 21 × 16.5 cm; **c** The J. Paul Getty Museum, *Initial G: Saint Blaise*, Ms. 73 (2003.87) recto, 15.7 × 12 cm; **d** The National Gallery of Art, Washington D.C., *Saint Lawrence (Initial D from a Choir Book (Gradual))*, 1948.11.12, 14.9 × 12.5 cm; **e** Burke collection, *Initial O with a Camaldolese Saint*, M2223.28, 15.0 × 12.7 cm; **f** McCarthy collection, *Initial G with The Nativity of the Virgin Mary,* 16569/BM1201, 19.4 × 12.6 cm

usually strictly restricted or disallowed altogether [20–22], and the analysis is therefore limited to non-invasive techniques.

Non-invasive analytical methods most typically used to study illuminated manuscripts include single-point and scanning XRF spectroscopy (MA-XRF), UV–vis-NIR-SWIR reflectance spectroscopy (FORS), Raman spectroscopy, and external reflection FT-IR spectroscopy [22]. To assess the practical limits of each of these methods for the detection of smalt in the presence of ultramarine and to better contextualize the manuscript data, a series of mock-up samples containing known mixtures of ultramarine and smalt painted on parchment were also analyzed. The study used a range of instruments housed at multiple institutions (see Additional file 3: Table S1) to determine which methods allow for the identification of smalt in the presence of ultramarine and the practical limitations of each technique. Finally, we will present an overall summary of the pigments present in the manuscript fragments and the degree of confidence in the assignment of smalt inferred from the preliminary findings [16, 17].

Materials and methods
15th-century Venetian manuscript fragments by the Murano Master
The six Master of the Murano Gradual manuscript pages analysed, shown in Fig. 1, are thought to belong to the now fragmented volumes mentioned in the Introduction. They are currently held in the collections of the Fitzwilliam Museum (Cambridge, UK), the National Gallery of Art (Washington, D.C.), The J. Paul Getty Museum (Los Angeles), and two private collections [23, 24] (see Additional file 3: Table S1 for details). The historiated initial *G* representing the *Dormition of the Virgin* shown in Fig. 1a, which prompted the investigation of the set, shows the Virgin Mary on her deathbed. Two other fragments depict narrative scenes, namely *The Nativity of the Virgin Mary* and a scene of Saint Jerome extracting a thorn from a lion's paw. The remaining three fragments include images of Saint Blaise, Saint Lawrence, and an unnamed Camaldolese Saint, each enclosed in a decorated initial. On the verso of many of the fragments, there are music staff lines painted with vermilion and music notes and text presumably executed in iron gall ink.

Ultramarine and smalt mock-up samples
A series of mock-up samples were prepared to test how well small amounts of smalt could be detected if mixed with ultramarine. Samples in which the ratio of ultramarine to smalt was varied systematically from 100% smalt to 100% ultramarine were painted onto parchment (William Cowley, Newport Pagnell, UK) using synthetic ultramarine and smalt (Kremer Pigmente GmbH & Co. KG, n. 45010 and n. 10000) bound in gum Arabic (Set 1). Most paint samples were applied with a brush as single layers containing admixtures of ultramarine and smalt in a way consistent with how an artist would have applied paint when making an illuminated manuscript; the thickness of

Ricciardi *et al. Heritage Science*   (2022) 10:38

Page 4 of 18

the layers was not measured. Images of the Set 1 mock-ups and the pigment mass percentages are presented as Additional file 1: Fig. S1a.

A further set of samples (Set 2) was prepared with the goal of establishing whether the ability to identify smalt in a mixture using FORS might be influenced by overall color saturation. Titanium white (Kremer) was added to the mixtures of synthetic ultramarine (Kremer n. 45010) and smalt (Natural Pigments n. 417-13); the samples were bound with an acrylic medium (Golden Acrylics) and painted on parchment. The paint samples were applied as single layers containing admixtures of ultramarine and smalt using a draw down bar technique to control the paint thickness. The thickness varied between approximately 0.7 to 1 mm after drying. Images of the Set 2 mock-ups and the pigment mass percentages are presented as Additional file 1: Fig. S1b.

Analytical methods
Four non-invasive analytical methods were used in this study. The spectroscopic methods applied to each manuscript fragment and mock-up set are listed in Additional file 3: Table S1.

UV–vis-NIR-SWIR reflectance spectroscopy (FORS, 350–2500 nm)
FORS spectra were collected using FieldSpec fiber optic spectroradiometers (FieldSpec 3, FieldSpec 4, and FieldSpec4 HiRes, ASD Inc., now part of Malvern Panalytical Ltd.). These spectrometers cover the spectral range of 350–2500 nm with a spectral sampling of 1.1–1.4 nm. The diffuse reflectance spectra were either collected normal to the artwork with the illumination source at 45 degrees from the normal, or with a bifurcated probe with separate optical fibers for illumination and detection. These two illumination/collection geometries produce similar reflection spectra although their absolute intensities may differ.

X-ray fluorescence (XRF) spectroscopy and scanning
Single point X-ray fluorescence (XRF) spectra were collected using the ARTAX micro-XRF spectrometer (Bruker Nano Analytics). The Set 1 mock-ups and the *Dormition of the Virgin* fragment were measured under the following conditions: Rhodium (Rh) X-ray tube with polycapillary optic at 50 kV and 600 μA, with an acquisition time of 200 s and a spot size of 0.65 mm. The fragments of *Saint Blaise, Saint Jerome, The Nativity of the Virgin Mary*, and the *Camaldolese Saint* were measured under the following conditions: Tungsten (W) X-ray tube at 50 kV and 600 μA, with an acquisition time of 200 s and a 0.65 mm pinhole collimator. The *Saint Lawrence* fragment was measured under the following conditions:

Rh X-ray tube with polycapillary optic at 50 kV and 200 μA, with an acquisition time of 100 s and a spot size of 0.06 mm. Single point XRF spectra of the Set 2 mock-ups were collected with the National Gallery of Art XRF system (described below) under the following conditions: Rh X-ray tube with polycapillary optic at 50 kV and 750 μA, with an acquisition time of 20 s and a spot size of 1 mm.

XRF area scans were collected with two different systems. *Saint Lawrence* was scanned with the National Gallery of Art custom system which consists of a 50 W Rh X-ray tube with a converging polycapillary optic (variable spot size from 0.1 to 1 mm, XOS), a 50 mm^2 silicon drift detector with a digital pulse processor (Vortex-90EX, SII DPP, Hitachi High Technologies Science America, Inc.), and a computer-controlled easel which moved the artwork during scanning (SmartDrive). The *Saint Lawrence* fragment was scanned under the following conditions: 50 kV and 750 μA, with an acquisition time of 100 ms, a spot size of 0.5 mm, and a speed of 5 mm/sec. For this fragment, data analysis utilized custom XRF fitting software developed at the National Gallery of Art and The George Washington University [25]. *Saint Jerome, Saint Blaise*, and *The Nativity of the Virgin Mary* were scanned at the GCI with a Bruker M6 Jetstream (Rh tube with pinhole collimator, operated at 50 kV, 600 μA, 120 (*Initial G with The Nativity of the Virgin Mary*) or 230 (*St. Blaise* and *St. Jerome*) μm spot size, 200 μm sampling and a dwell time of 10 ms/pixel) was used. Data analysis of these fragments utilized the Datamuncher [26] and PyMCA [27, 28] software suites.

XRF linescans of the Set 2 mock-ups were also collected with the National Gallery of Art custom system, like above but with a different detector and pulse processor (Amptek 50 mm^2 silicon drift detector and a Dante-XG Labs digital pulse processor). The mock-ups were scanned under the following conditions: 50 kV and 200 μA, with an acquisition time of 10 s, and an X-ray spot size of 0.1 mm and a step size of 0.1 mm. A XRF linescan of the *Saint Lawrence* fragment was collected with the ARTAX micro-XRF spectrometer (Bruker Nano Analytics) and measured under the following conditions: Rh X-ray tube with polycapillary optic at 50 kV and 200 μA, with an acquisition time of 100 s, and a X-ray spot size of 0.06 mm and a step size of 0.1 mm.

Raman spectroscopy
Raman spectra were collected on the Set 1 mock-ups and some of the fragments using an inVia confocal Raman microscope (Renishaw Inc.), equipped with a 785 nm diode laser. The spectrometer was wavenumber calibrated using a silicon standard (520.5 cm^{-1}). For the mock-ups, fifteen spectra (10–30 s accumulation

Ricciardi *et al. Heritage Science*   (2022) 10:38

Page 5 of 18

time each) were averaged for each acquisition. Single spectra were collected on the manuscript fragments to reduce the amount of laser light exposure to the objects. All analyses were carried out using a $50 \times$ achromatic long-focus microscope objective (Leica Microsystems) on areas measuring approximately 2×20 μm. The laser power density at the surface of the objects was adjusted as needed to prevent damage to the pigments, and was always less than 0.05 mW/μm^2.

Fourier-transform infrared (FT-IR) spectroscopy

Mid-infrared spectra of the Set 1 mock-ups and some of the manuscripts were collected with a portable ALPHA FT-IR spectrometer (Bruker Optics) operated in external reflection mode (ER-FTIR). Spectra were collected over the 6000–400 cm^{-1} range, with a resolution of 4 cm^{-1}, averaging 80 scans per spectrum. The investigated area was around 20 mm^2. The spectra were processed using a smoothing algorithm included in the spectral acquisition software. They show the typical distortions due to the derivative shape, Reststrahlen effect and intensity enhancement as a consequence of the optical properties of the investigated substrates.
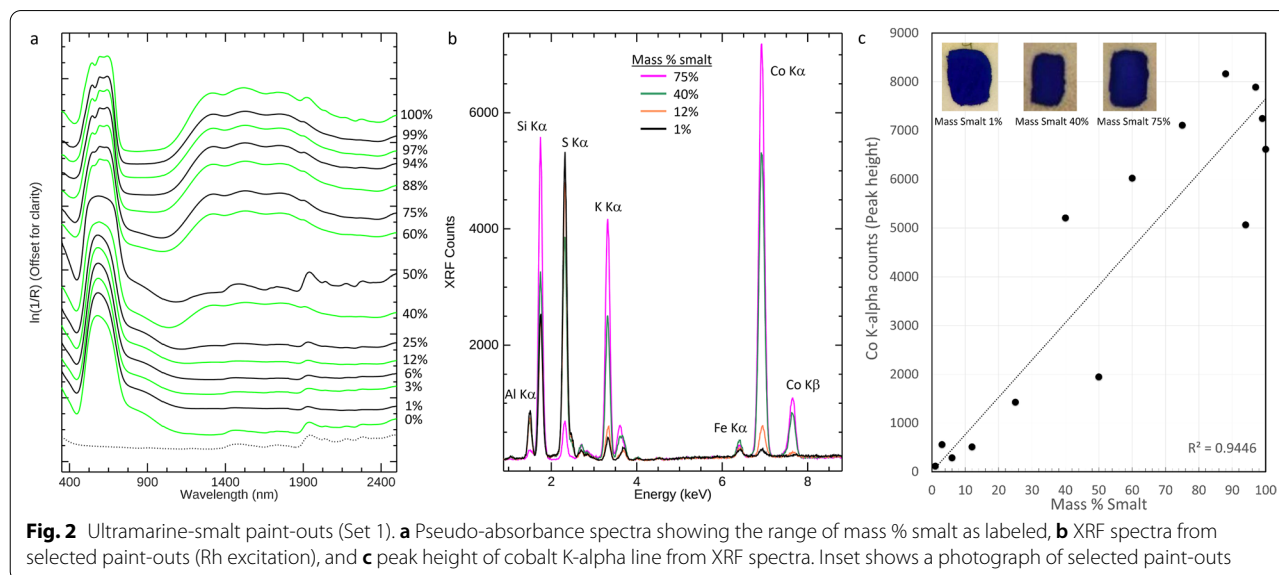
Results and discussion
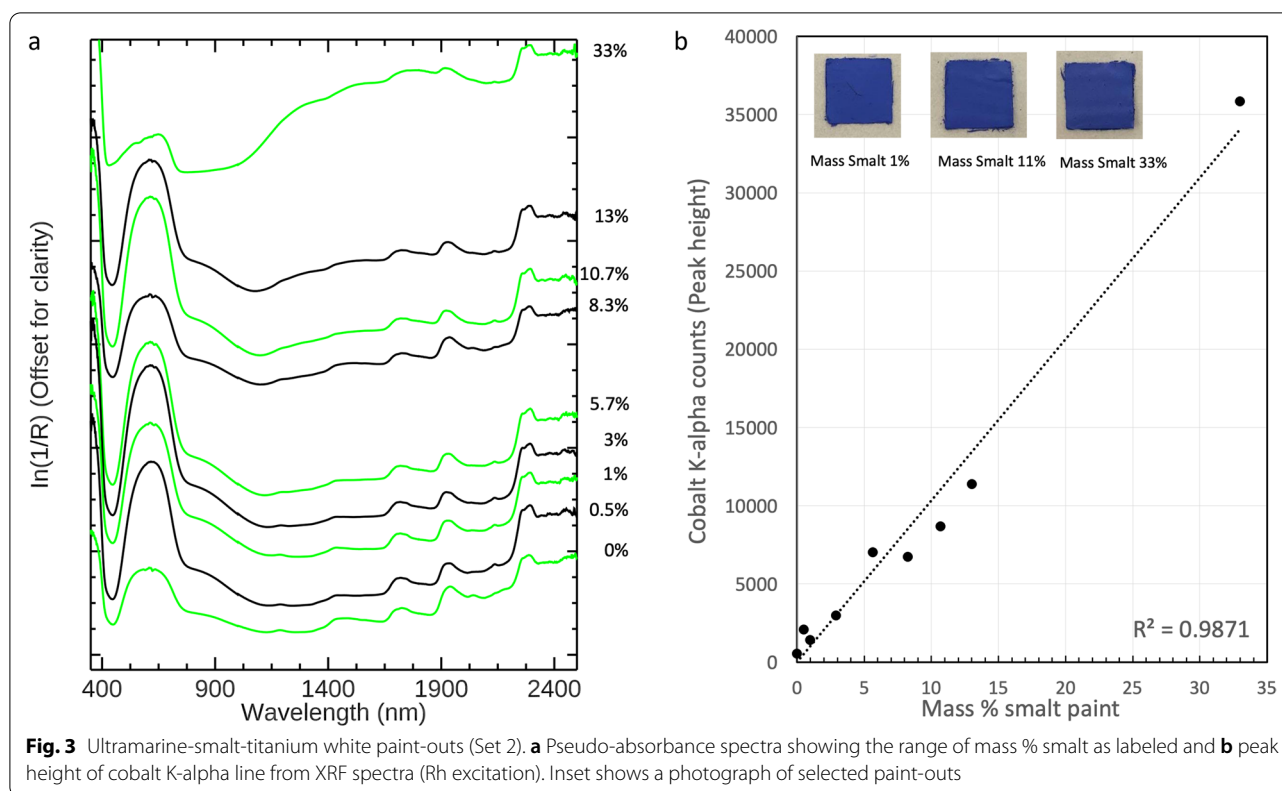### Summary of results obtained on the mock-up samples

The prepared mock-up paint samples described in "Ultramarine and smalt mock-up samples" section were examined using FORS, XRF, Raman, and FTIR. The goal of this analysis was to approximate how much smalt would need to be incorporated into ultramarine (with and without an added white pigment) to be detected by each method.

FORS analysis of mock-up samples

The key goal of reflectance spectral analysis was to determine how much smalt (mass percent of smalt pigment/paint) in the presence of ultramarine is required before the characteristic smalt absorption features can be distinguished from those of ultramarine. Briefly, in the visible spectral region, smalt absorbs from ~490 to 700 nm due to ligand field transitions, with absorption sub-bands near 545, 595, and 645 nm. A broad near-infrared absorption is also present from ~1150 to 2000 nm, with sub-bands near 1315, 1525, and 1780 nm [29, 30]. For ultramarine, only a broad absorption centered near 600 nm associated with a charge transfer transition is present [30]. Ultramarine has no near-infrared absorptions.

Reflectance spectra of each of the mock-up samples were collected from 350 to 2500 nm and were converted to absorbance by calculating natural log(1/reflectance). Figure 2a shows absorption spectra of the mock-up samples in Set 1 and Fig. 3a the absorption spectra of the mock-up samples in Set 2. The Set 1 mock-ups consists of paint-outs of synthetic ultramarine mixed with smalt on parchment while Set 2 mock-ups include a white pigment (titanium white). In general, the absorption spectra from the two data sets reveal clear changes as the mass percentage of smalt increases, but only at high percentages (greater than ~33–40%). In Set 1 (Fig. 2a), when only ultramarine is present, the absorption near 600 nm has a Gaussian shape. In contrast, when only smalt is present, the broad absorption has an overall shape that is more rectangular than Gaussian, with smalt's absorption sub-bands easily discernible. As the mass percentage of smalt increases, the dominant absorption band in the visible spectral region becomes more rectangular in

Fig. 2 Ultramarine-smalt paint-outs (Set 1). **a** Pseudo-absorbance spectra showing the range of mass % smalt as labeled, **b** XRF spectra from selected paint-outs (Rh excitation), and **c** peak height of cobalt K-alpha line from XRF spectra. Inset shows a photograph of selected paint-outs

Ricciardi *et al. Heritage Science*   (2022) 10:38

Page 6 of 18

Fig. 3 Ultramarine-smalt-titanium white paint-outs (Set 2). **a** Pseudo-absorbance spectra showing the range of mass % smalt as labeled and **b** peak height of cobalt K-alpha line from XRF spectra (Rh excitation). Inset shows a photograph of selected paint-outs

shape (~40–50% smalt and above), and at higher mass percentages of smalt the visible absorption sub-bands are observed (75% smalt and above). In the near-infrared, a similar trend is observed as in the visible spectral region, namely that the broad near-infrared absorption and associated sub-bands become apparent at smalt concentrations above ~40%. Characteristic absorption features of smalt start to become apparent by ~40% and become dominant by ~75%.

In the Set 2 mock-ups Fig. 3a, a white scattering pigment (titanium white) was introduced into the ultramarine-smalt mixture to effectively increase the optical path. The addition of the white pigment also serves as a proxy for the light blue areas of the illuminated manuscript fragments. Overall, the absorption spectra of the Set 2 mock-ups follow the same trend as the Set 1 mock-ups, although the smalt absorption features were detected at approximately a 10% lower mass percent of smalt paint (i.e. smalt detected at 33%).

XRF analysis of mock-up samples
Point XRF was performed on both sets of mock-ups. In Fig. 2b, representative XRF spectra are shown from a selected set of paint swatches in the Set 1 mock-ups. In these spectra, as the mass percentage of smalt increases the intensity of the Co Kα (6.93 keV) and Co Kβ

(7.65 keV) emission lines also increase. The XRF spectra also show the Fe Kα emission line at 6.4 keV. The Fe Kβ line (whose intensity is a fraction of the Fe Kα occurs at 7.06 keV. Although the Fe Kα line and Co Kα line overlap, the Fe Kβ contribution is not significant to the estimate of the Co Kα in the mock-ups. Plots of the peak intensity of the Co Kα line from the Set 1 (Fig. 2c) and Set 2 (Fig. 3b) mock-ups show an increase with the mass percentage of smalt. XRF measures the total amount of cobalt present and as such is sensitive to the concentration (% smalt) and the paint layer thickness. The paint layer thickness was more carefully controlled in the Set 2 mock-ups, and as a result, the correlation is more linear. The XRF data suggests that in these mock-ups, the presence of cobalt can be detected down to the 1% level.

Additionally in these samples, careful examination of the Si and Al XRF signal provides some indirect indication of the presence of smalt (as described in Additional file 2: Fig. S2), and may warrant further research.

FTIR and Raman spectroscopy of mock-up samples
Molecular spectroscopy by FT-IR has been used to identify both ultramarine and smalt in works of art [31–33]. Ultramarine has three characteristic bands between 550 and 700 cm^{-1}. Two of them are due to the stretching of aluminium-oxygen bonds (652 and 686 cm^{-1}), and

Ricciardi *et al. Heritage Science*   (2022) 10:38

Page 7 of 18

the other (578 cm^{-1}) to the sulphur ions. As shown in Fig. 4, these bands disappear as the content of ultramarine drops below ~ 50%. Both ultramarine and smalt are characterized by the antisymmetric stretching mode of the silicon-oxygen-silicon (Si–O–Si) bond between 1000 and 1100 cm^{-1} [34]. As shown in Fig. 4, the position of this band shifts by about 80 cm^{-1} between ultramarine and smalt. While this appears promising for signaling the presence of smalt in the presence of ultramarine, the absolute band position is variable by as much as 33 cm^{-1} [35], which limits the robustness of this technique.

Raman spectroscopy is also commonly used in the examination of illuminated manuscripts for the molecularly-specific identification of mineral-derived pigments [36, 37]. Ultramarine is identifiable by the characteristic 549 cm^{-1} (S$_3^-$ v_1) band [38]. The signal typically associated with smalt is the Si–O stretch at 463 cm^{-1} [39, 40], but this stretch is also present in other silica-containing materials, and thus is not a unique identifying band for smalt. Raman spectra of the Set 1 mock-ups (Fig. 5) always show the presence of the 549 cm^{-1} band when ultramarine is present; the 463 cm^{-1} Si–O stretch is visible only in pure smalt and in the 50% smalt mixtures (Fig. 5, inset). While generally a powerful tool for pigment analysis, Raman spectroscopy is therefore unlikely to unambiguously identify the presence of small quantities of smalt in

ultramarine mixtures, and, due to its relatively surface-specific nature, would not be expected to detect smalt used as an underlayer.

Comparison of non-invasive methods to detect smalt in the presence of ultramarine

Of the four methods used on the mock-ups—one elemental (XRF) and three molecular (FORS, FTIR, Raman)—XRF provides the highest detectability. With XRF, the presence of cobalt was detected at the 1% level of smalt in ultramarine (by mass). Molecular identification of smalt is the most robust with FORS (reflectance spectroscopy) due to smalt's unique absorptions in the visible and near-infrared spectral regions. Some of these unique absorption features were observed when the smalt concentration was as low as 30–40%. The challenge for Raman spectroscopy for identifying smalt/ultramarine mixtures is the lack of a unique marker for smalt. The difficulty for FTIR is that the same band (Si–O–Si) is used for identification of both smalt and ultramarine. As a result, in the remainder of this paper, only XRF and FORS results are presented in order to better understand the distribution in the ultramarine regions of the illuminated manuscript fragments, and to roughly estimate the amount of smalt present in these objects.
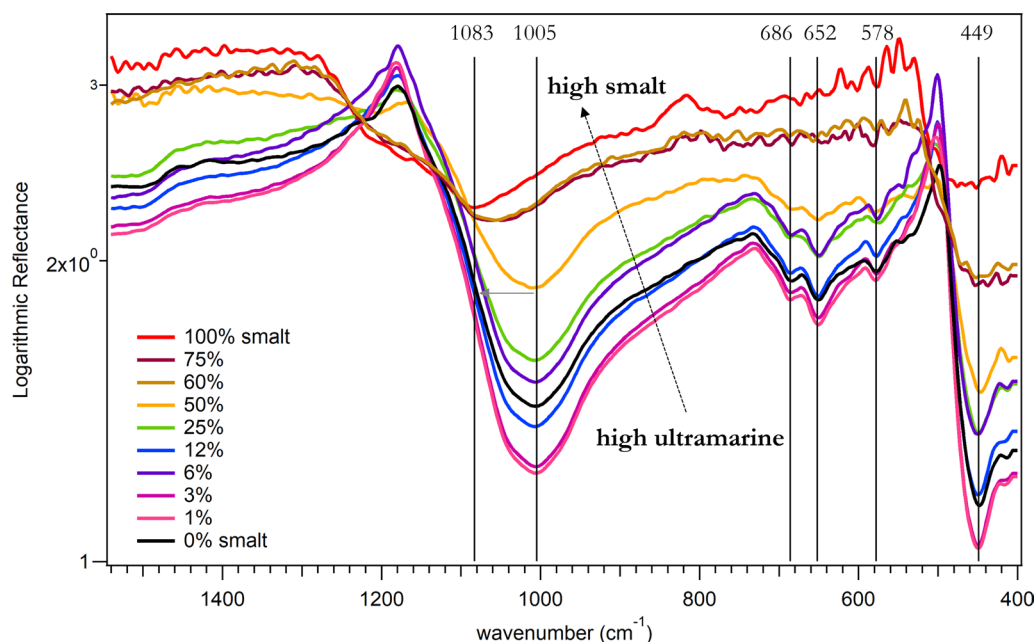

Fig. 4 Detail of ER FT-IR spectra of selected samples (1500–400 cm^{-1}). The indicated bands at 1083 and 1005 cm^{-1} are Si–O–Si (antisymm stretching); bands at 686 and 652 cm^{-1} are Al–O stretching; band at 578 cm^{-1} is the S$_3^-$ feature of ultramarine; the band at 449 cm^{-1} is silicate

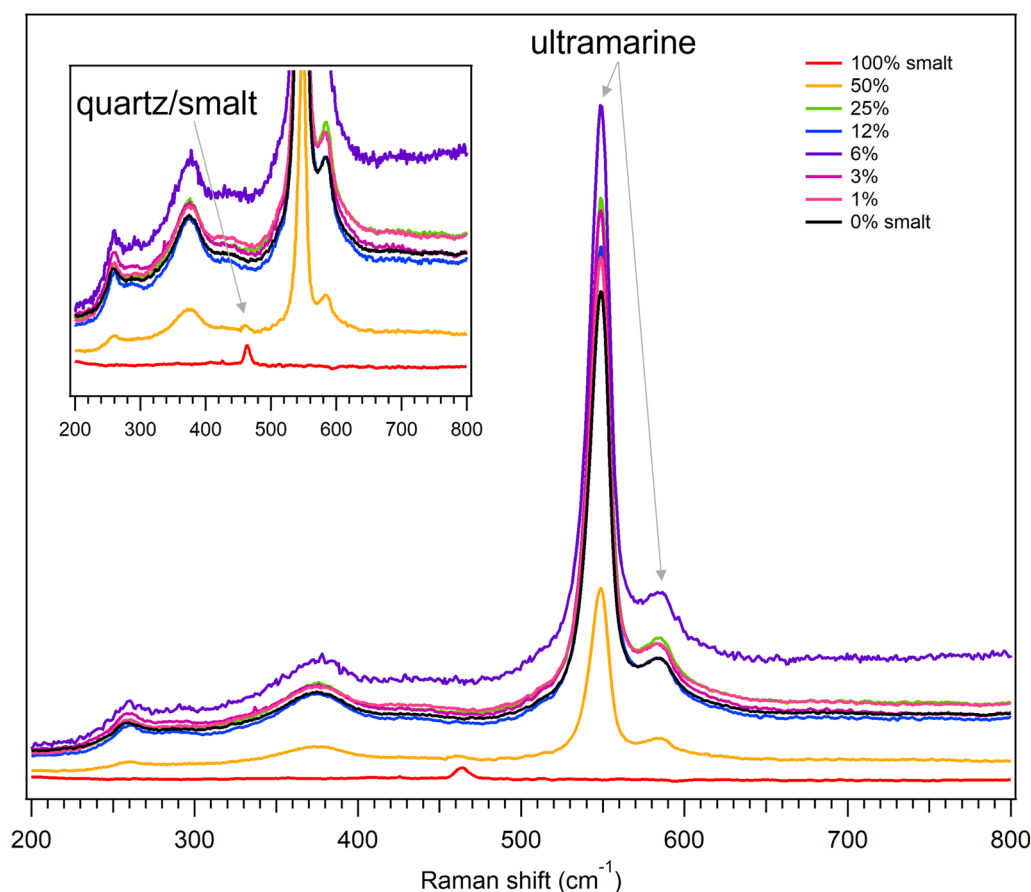Ricciardi *et al. Heritage Science*　　(2022) 10:38

Page 8 of 18

Fig. 5 Raman spectra of selected samples (200–800 cm^{-1})

Summary of non-invasive results obtained on the illuminated manuscript fragments

The results of the non-invasive methods, including point XRF and FORS measurements on all the fragments and XRF scanning on two of the fragments, are discussed below.
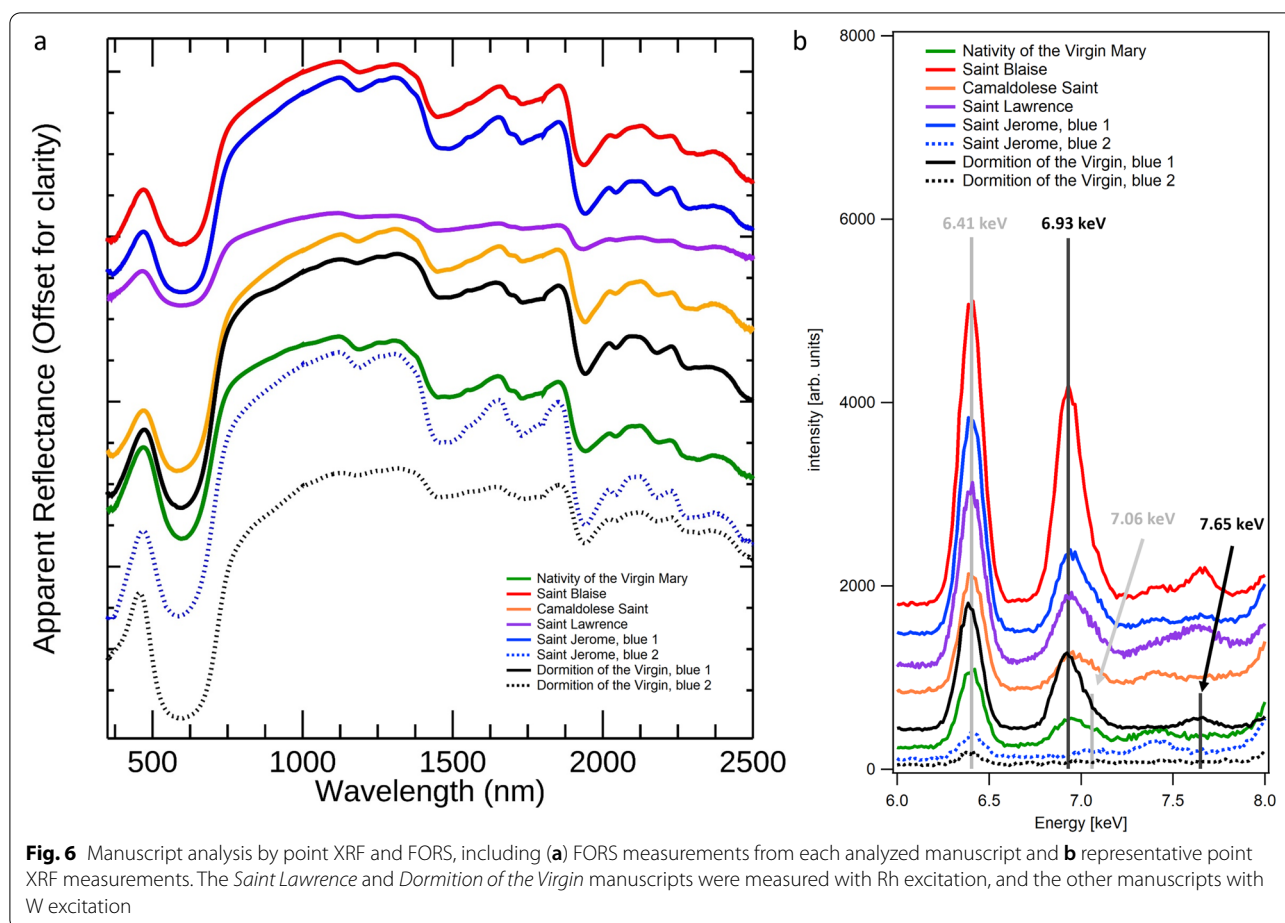
Point XRF and FORS of all the fragments in the blue areas

Representative FORS and XRF spectra from blue areas in each manuscript fragment are shown in Fig. 6. All of the blue passages in each fragment, within the main scene and also in the surrounding decorations, showed evidence for ultramarine identified primarily based on spectral features in the reflectance spectra as shown in Fig. 6a coupled with the detection of aluminium and silicon by XRF. Many of the blue areas also showed evidence for cobalt in the XRF spectra, although no absorption features associated with smalt were detected in the FORS spectra.

All of the FORS spectra in Fig. 6a show characteristic features of ultramarine, including a narrow reflectance peak between ~450–470 nm, a strong absorption

at 600 nm followed by a steep increase in reflectance at approximately 700 nm, and no other features out to 2500 nm. None of the characteristic absorption bands for smalt were detected in the visible or near-infrared spectral regions. Table 1 characterizes all of the blue areas analyzed for the six manuscript fragments, and in each case only evidence for ultramarine was found with FORS analysis.

The results from point XRF measurements in the blue passages (see Table 1) not only revealed the presence of elements associated with ultramarine (Al, Si, and K, with K present as a by-product of the purification process in natural ultramarine), but also iron and cobalt in many areas as shown in Fig. 6b. The spectra show an Fe Kα emission peak at 6.41 keV and a Co Kα peak at 6.93 keV, along with a shoulder on this cobalt peak at 7.06 eV which is the Fe Kβ emission. In cases where the Co Kα peak is intense, the Co Kβ is visible at 7.65 keV. In the light blue border in *Saint Blaise*, a blue area in *Saint Lawrence*, and the dark blue text background outside the initial in *Dormition of the Virgin*, both the Co Kα and Co Kβ lines were detected. Only the cobalt Kα lines were detected for the

Fig. 6 Manuscript analysis by point XRF and FORS, including (**a**) FORS measurements from each analyzed manuscript and **b** representative point XRF measurements. The *Saint Lawrence* and *Dormition of the Virgin* manuscripts were measured with Rh excitation, and the other manuscripts with W excitation

blue robe in *Initial G with Nativity of the Virgin Mary,* the dark blue in the initial in the *Camaldolese Saint,* and the dark blue border in *Saint Jerome.* In select areas of blue paint in *Saint Jerome* (the blue of Jerome's robe) and *Dormition of the Virgin* (the Virgin's dark blue robe), no cobalt was detected, and far less iron was detected as well (Fig. 6b, dashed traces). The XRF data suggests that the presence of cobalt and iron may be correlated in the blue areas, especially for *Saint Jerome.* Iron has been detected in the parchment, and thus XRF scanning is important to confirm the correlation between cobalt and iron.

XRF scanning of two illuminated manuscript fragments
To determine the distribution of cobalt in the ultramarine blue passages and whether it is correlated with iron, additional XRF scanning was performed on four of the manuscripts (see Additional file 3: Table S1). The analysis of the XRF data cube collected from *Saint Lawrence,* which involved fitting the individual XRF spectra to account for the partially overlapping cobalt Kα and iron Kβ emissions, produced maps of both cobalt Kα and Kβ emission lines (Fig. 7). In *Saint Lawrence,* Figs. 7b and e show that
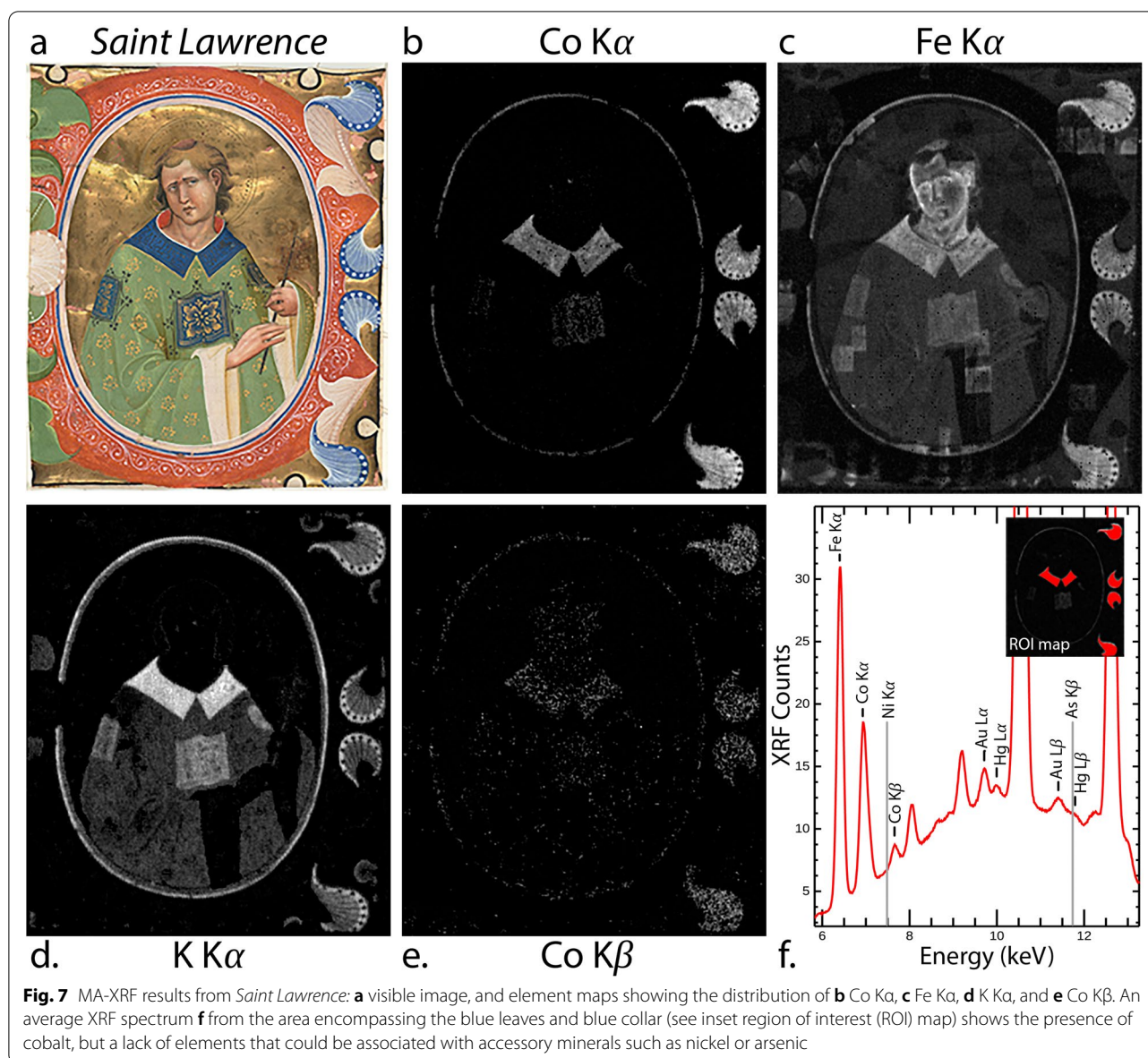
the cobalt Kα and Kβ emission maps coincide with all of the blue passages in the main scene and also in the surrounding decoration. That said, the cobalt distribution does not exactly follow the intensity of the blue color in the fragment. For example, the highest abundance of cobalt is in the light blue top and bottom leaves, and the lowest abundance of cobalt is in the dark blue emblem at the center of the robe. In contrast, the amount of potassium does mirror the visual intensity/hue of the blue (see K Kα map in Fig. 7d). For example, the areas that have the most potassium correspond with the darkest blue areas, like the blue collar and the edge of the leaves in the marginalia. Since potassium is associated with natural ultramarine as a result of the purification process, it is perhaps not surprising that its distribution follows that of ultramarine, the pigment FORS suggests is the dominant colorant. Since potassium is also a constituent of smalt, it cannot be ruled out that some of the potassium may be due to smalt.

Other elements commonly found with smalt besides cobalt include nickel and arsenic, which are associated with some cobalt ores. These elements were not detected

Ricciardi *et al. Heritage Science*   (2022) 10:38

Page 10 of 18

Table 1 Summary of FORS and XRF results obtained on the blue areas of the illuminated manuscript fragments analyzed

Title	Area	'Inside'	'Outside'	FORS	XRF—Major, minor, (trace) signal	Pigments
Dormition of the Virgin	Initial G		✓	max refl 476 nm, min refl 600 nm, abs 1452 nm	**Si**, **Pb**, K, Al, Fe, Co, S (Cu, Ti, Mg, Na)	Ultramarine, smalt, lead white
	Background to text		✓	max refl 462 nm, min refl 600 nm	**Si**, Pb, K, Fe, Al, Co, S, Cl? (Ti, Mg, Na)	Ultramarine, smalt, lead white
	Sky	✓		max refl 471 nm, min refl 594 nm	**Pb**, Si, Al, K, Fe, Co, (Na, Mg, Ti)	Ultramarine, smalt, lead white
	Book	✓		n/a	**Si**, **Pb**, K, Al, Cl? (Na)	Ultramarine, lead white
	Virgin's robe	✓		max refl 455 nm, min refl 600 nm, abs band 1452 nm	**Pb**, **Si**, K, Al, Cl? (Na, Ti?)	Ultramarine, lead white
St Blaise	Dark blue in border		✓	max refl 469 nm, min refl 597 nm, slight abs 1450 nm	**Pb**, Fe, Co, K, Si, (Ti, As, Al?)	Ultramarine, smalt, lead white
	Light blue in border		✓	max refl 471 nm, min refl 594 nm	**Pb**, Fe, Co, Al, Si (K?, Ti?)	Ultramarine, smalt, lead white
	Dark blue in robe	✓		max refl 469 nm, min refl 593 nm	**Pb**, Fe, Co, K, Si (Ti)	Ultramarine, smalt, lead white
	Light blue in robe	✓		max refl 468 nm, min refl 594 nm, abs 1452 nm	**Pb**, Fe, Co, K, Si, Hg, (Ti?)	Ultramarine, smalt, lead white, vermilion (likely on verso)
	Blue on glove	✓		n/a	**Pb**, Fe, Co, K (Ti)	Ultramarine, smalt, lead white
St Jerome	Dark blue in border		✓	max refl 470 nm, min refl 597 nm	**Pb**, Fe. Co, K, Si (Al, Ti)	Ultramarine, smalt, lead white
	Light blue in border		✓	max refl 465 nm, min refl 597 nm, slight abs 1451 nm	**Pb**, Fe. Co, K, Si (Ti)	Ultramarine, smalt, lead white
	Jerome's robe lining	✓		max refl 468 nm, min refl 584 nm, abs 1451 nm	**Pb**, K, Si	Ultramarine, lead white
St Lawrence	Dark blue in border		✓	max refl 466 nm, min refl 595 nm, refl inflection 711 nm, abs 1451 nm	**Pb**, Fe, Ca, Co, K, Au, Hg, Si (Cu, Ti)	Ultramarine, smalt, lead white
	Light blue in border		✓	max refl 469 nm, min refl 595 nm, refl inflection 700 nm	**Pb**, Fe, Co, Ca, K, Cu, Si	Ultramarine, smalt, lead white
	Dark blue collar	✓		max refl 470 nm, min refl 601 nm, refl inflection 711 nm	**Ca**, Fe, Ag, Co, K, Si (Cu, Pb, Ti)	Ultramarine, smalt, silver
	Dark blue robe design	✓		max refl 488 nm, min refl 590 nm, refl inflection 695 nm	**Cu**, Ca, Fe, K, Au, Hg, Co, Si (Pb, Ti)	Ultramarine, smalt, gold on copper green
Initial G with The Nativity of the Virgin Mary	Dark blue in border		✓	max refl 466 nm, min refl 592 nm, abs 1451 nm	**Pb**, K, Fe, Co, Si (Ti, Mn, Al); one spot with **Hg** from nearby red field	Ultramarine, smalt, lead white
	Light blue in initial		✓	n/a	**Pb**, Fe, Co, K, Si (Ti); **Hg** (one spot)	Ultramarine, smalt, lead white (vermilion likely from verso)
	Virgin's robe	✓		max refl 465 nm, min refl 597 nm, abs 1451 nm	**Pb**, Fe, Co, K, Si (Ti, Sn?)	Ultramarine, smalt, lead white
Camaldolese Saint	Dark blue of initial		✓	max refl 469 nm, min refl 583 nm, slight abs 1449 nm	**Pb**, K, Co, Si (Al, Ti)	Ultramarine, smalt, lead white
	Light blue of initial		✓	n/a	**Pb**, **Hg,** K, Co, Si (Al)	Ultramarine, smalt, lead white (vermilion likely from verso)

Reflectance spectral features and chemical elements due solely to the parchment support are not listed

Ricciardi *et al. Heritage Science*   (2022) 10:38

Page 11 of 18

Fig. 7 MA-XRF results from *Saint Lawrence:* **a** visible image, and element maps showing the distribution of **b** Co Kα, **c** Fe Kα, **d** K Kα, and **e** Co Kβ. An average XRF spectrum **f** from the area encompassing the blue leaves and blue collar (see inset region of interest (ROI) map) shows the presence of cobalt, but a lack of elements that could be associated with accessory minerals such as nickel or arsenic

in the *Saint Lawrence* manuscript, even after averaging the XRF spectra from the blue collar and blue leaves (Fig. 7f). Interestingly, the XRF map for Fe Kα of *Saint Lawrence* (Fig. 7c) shows iron is distributed throughout all of the blue areas, in addition to being present in the fleshtones, in square shapes that likely correspond with musical notation on the verso of the manuscript, and in trace amounts in the background. The maps provide clear evidence that the cobalt and iron are correlated in the blue areas and are therefore both likely to be found in the pigment/pigment mixture.

The XRF maps for *Saint Jerome* are shown in Fig. 8 and were collected under different conditions than that for *Saint Lawrence*. Specifically, the acquisition time per

pixel were shorter than those for *Saint Lawrence*, and thus the XRF signal intensities were lower. The strongest cobalt signals are in the blue leaves at upper left and right, and no cobalt was detected in the light blue robe of *Saint Jerome*. The leaves contain lighter blue and darker blue areas, and both areas have potassium, cobalt, and iron. The intensity difference in the potassium map between the light and dark blue areas is more pronounced than in the cobalt and iron maps, similar to what was observed for the *Saint Lawrence* fragment.

XRF linescans of Set 2 mock-ups and Saint Lawrence
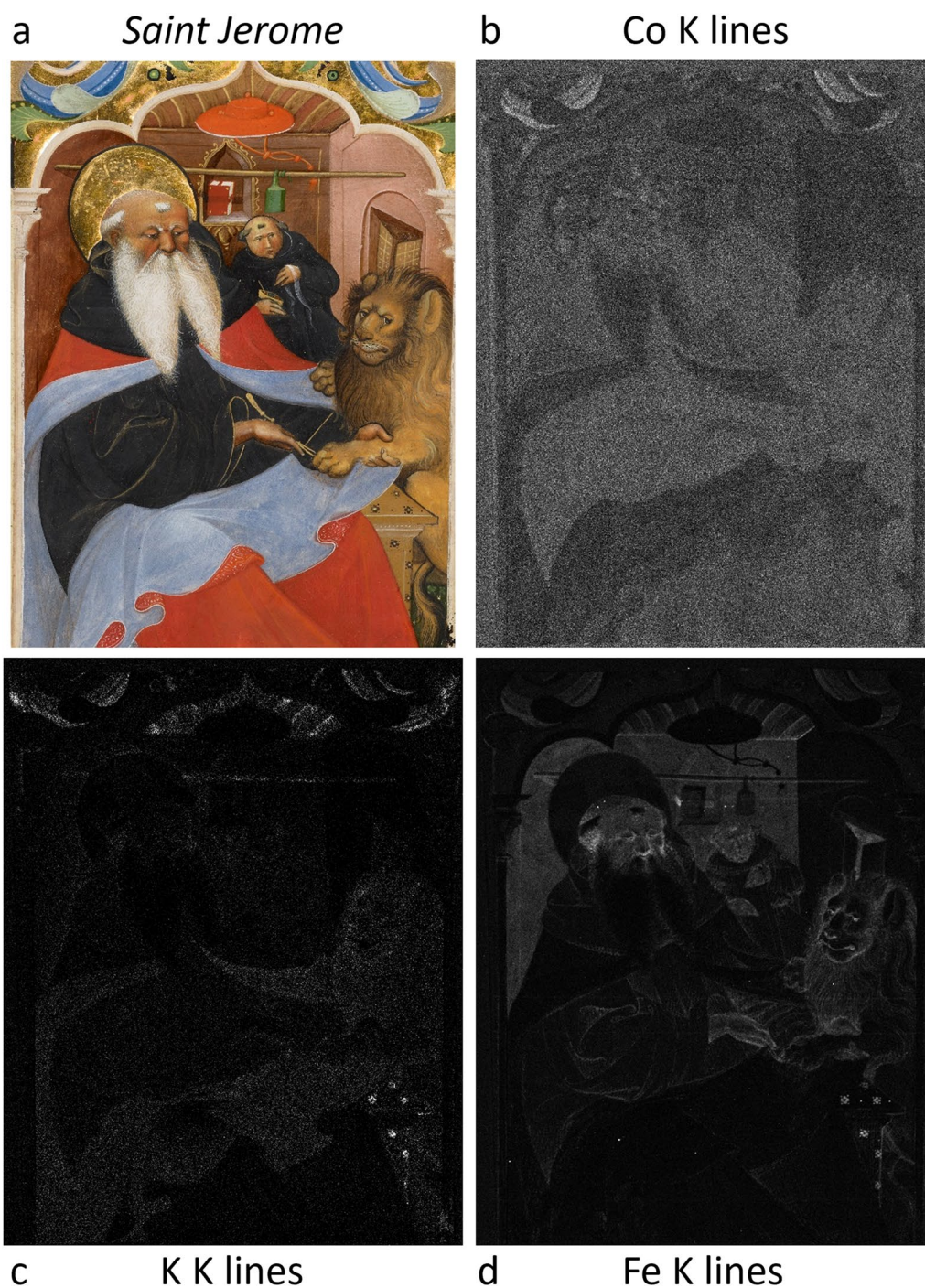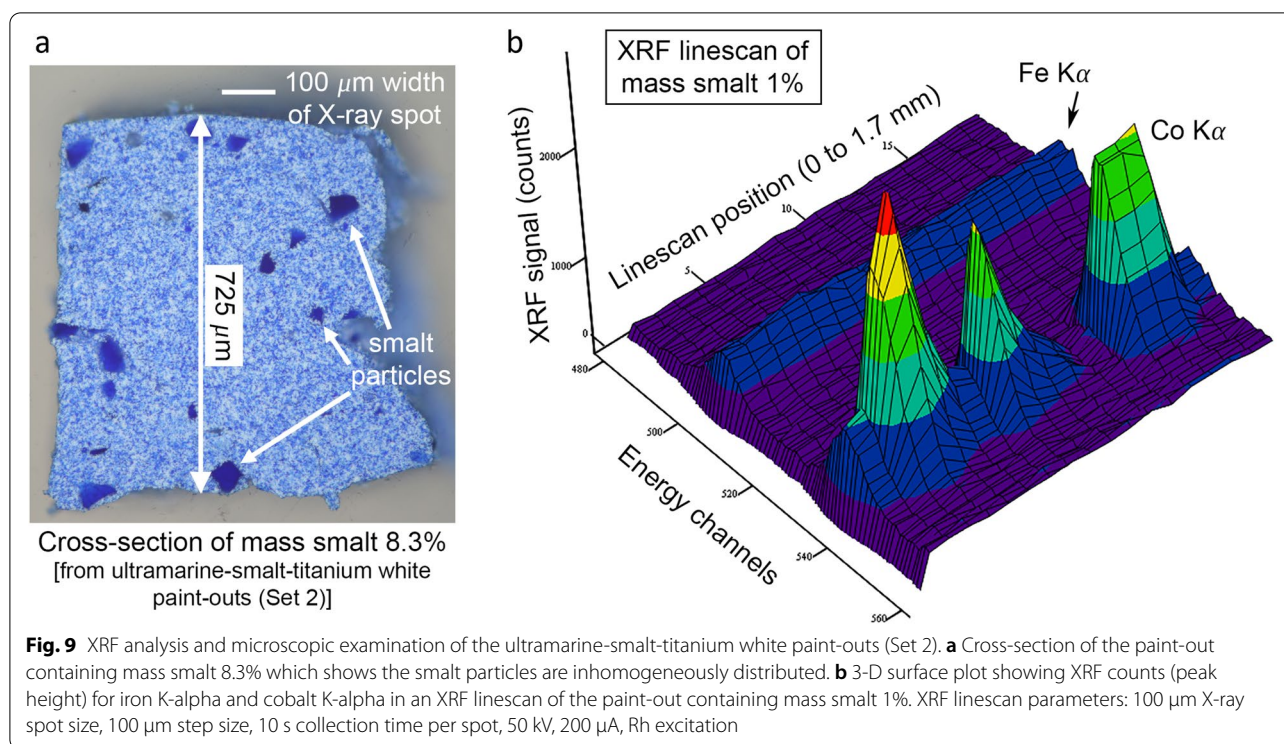Typically, following the grinding required to prepare pigments, the pigment particle size of smalt is larger than

Fig. 8 MA-XRF results from *Saint Jerome:* **a** Visible image, and element maps showing the distribution of **b** Co, **c** K, and **d** Fe. For all element distributions, the Kα and Kβ lines have been examined together during fitting in PyMCA

that of ultramarine. For example, in the Set 2 mock-ups, the smalt used had a mean particle size of 40 μm whereas the synthetic ultramarine had a mean particle size of 2.5 μm, according to the suppliers. A cross-section of the Set 2 mock-up sample containing 8.3% smalt is shown in

Fig. 9a and the difference in particle size is readily apparent, with large dark blue smalt particles visibly scattered in a matrix of finely ground ultramarine. Because the size of the smalt particles is large and the concentration by mass in the sample is low, there is significant separation
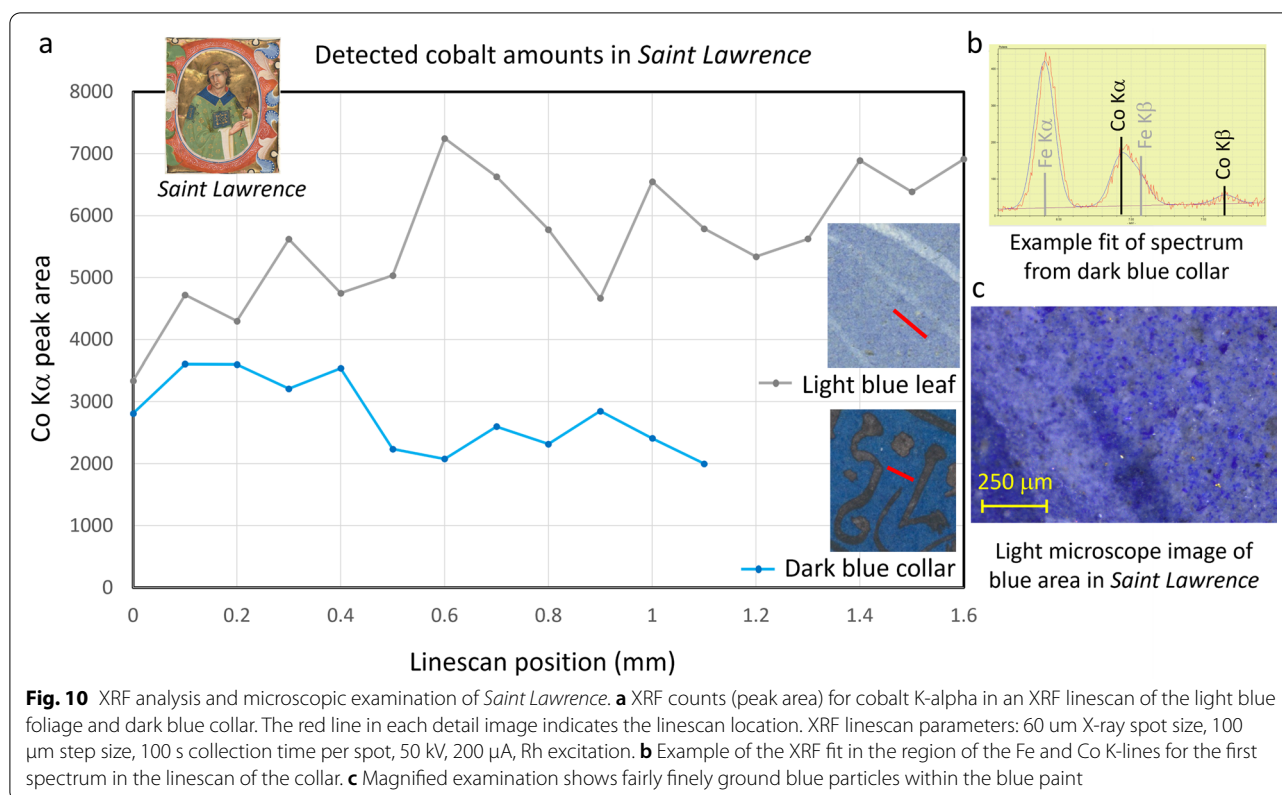
Ricciardi *et al. Heritage Science*   (2022) 10:38

Page 13 of 18

Fig. 9 XRF analysis and microscopic examination of the ultramarine-smalt-titanium white paint-outs (Set 2). **a** Cross-section of the paint-out containing mass smalt 8.3% which shows the smalt particles are inhomogeneously distributed. **b** 3-D surface plot showing XRF counts (peak height) for iron K-alpha and cobalt K-alpha in an XRF linescan of the paint-out containing mass smalt 1%. XRF linescan parameters: 100 μm X-ray spot size, 100 μm step size, 10 s collection time per spot, 50 kV, 200 μA, Rh excitation

between many of the individual smalt particles. This size difference between ultramarine and smalt, especially at the low smalt concentrations, can be exploited to look for individual smalt particles by XRF scanning with a small X-ray spot size. This can be seen from a 3-D plot of a 1700 μm linescan of a less concentrated smalt sample (1%) than the 8.3% sample shown in Fig. 9a. This linescan (Fig. 9b) used a 100 μm X-ray spot size with a step size of 100 μm and a longer acquisition time than what was used for area scanning. Along this linescan, the Co Kα peak height changes in intensity from baseline to ~ 2500 counts and shows three maxima, whereas the peak height for Fe Kα remains relatively constant. Given that the cross-section shown in Fig. 9a is nearly 1 mm thick, signal may originate from smalt particles at the paint surface as well as those in the volume below the XRF spot. We therefore interpret each cobalt maxima in the linescan as coming from one to a few discrete smalt particles.

Two analogous linescans in the upper light blue leaf and the dark blue collar of the *Saint Lawrence* fragment—areas known to contain cobalt based on the Co XRF maps in Fig. 7—were also collected and are shown in Fig. 10a. These linescans show a distinctly different pattern than that shown in Fig. 9. While the cobalt signal (peak area) does vary over the length of the scans, it never drops to zero (baseline), and no discrete maxima are apparent. Unlike the case of the mockup, there is no evidence in the linescans for the presence of scattered

discrete smalt particles. Because the iron signal is larger in the fragments than in the mock-ups, the Co Kα and Fe Kβ signals were separated with deconvolution (an example fit is shown in Fig. 10b). In these linescans, a spot size of 60 μm was used, and the paint layer is expected to be under 100 μm thick. Thus, if Co-rich particles of the relatively large size typical of smalt existed in these areas, we would have expected to detect them in the linescans by seeing discrete maxima as was true for the mock-up. Magnified examination of blue areas in *Saint Lawrence* (see example of a light microscope image in Fig. 10c) did not reveal larger particles with morphologies typical of smalt (i.e. glassy shards).

Implications for smalt in ultramarine blue passages of the illuminated manuscript fragments

The analysis of the mock-up samples presented here along with the data collected from the six fragments allows some additional information about the manuscripts to be inferred. The data from the mock-ups indicates that above ~ 30% smalt in ultramarine, the FORS measurements would likely betray the presence of smalt, which is not observed in the data from the fragments. This leads to the conclusion that if the cobalt is present as smalt in the fragments, then smalt must be less than ~ 30% relative to ultramarine by mass. Unfortunately at this concentration, it is not possible to confirm that cobalt is present as smalt by the molecular spectroscopy techniques used

Fig. 10 XRF analysis and microscopic examination of *Saint Lawrence*. **a** XRF counts (peak area) for cobalt K-alpha in an XRF linescan of the light blue foliage and dark blue collar. The red line in each detail image indicates the linescan location. XRF linescan parameters: 60 um X-ray spot size, 100 µm step size, 100 s collection time per spot, 50 kV, 200 µA, Rh excitation. **b** Example of the XRF fit in the region of the Fe and Co K-lines for the first spectrum in the linescan of the collar. **c** Magnified examination shows fairly finely ground blue particles within the blue paint

here. XRF, of course, can identify additional elements that may be associated with the cobalt ore used in smalt production, such as arsenic and nickel, which are commonly found in 17th and 18th century paintings containing smalt [11, 12]. Recent research by Stege has expanded on this by examining smalt-containing paintings from the 15th century, identifying additional elements associated with cobalt ores such as iron [15]. With the exception of one instance (a portion of the dark blue border in *Saint Blaise*), arsenic and nickel were not found in the fragments studied here, but as noted above and in Table 1, iron is present in all of cobalt-containing blue fields, with the exception of the fragment *Camaldolese Saint*. This raises the intriguing prospect that the co-localization of cobalt and iron in the fragments may further support the inference that cobalt is indeed present as smalt, derived from a cobalt source containing iron [15].

High spatial resolution (less than 100 µm spot size), high-sensitivity XRF offers the opportunity to explore the size of the Co-rich particles in the fragments. Because of smalt's low tinting strength, smalt is characterized by its relatively large particle size (~ 40 µm) in comparison to ultramarine. In this work, we demonstrated that linescanning with a 100 µm spot size detected cobalt within discrete smalt particles in ultramarine-smalt-titanium white mixtures. It was a surprise, then, that in the *Saint Lawrence* fragment cobalt was detected continuously rather than as a fluctuating cobalt intensity that could be attributed to coarsely ground smalt particles. One possible explanation for this is that the smalt was finely ground in the fragment, and more evenly distributed within the paint film than was the case in the mock-ups. An example in support of this is the finding by Spring et al. of finely ground smalt particles (6–15 µm) in a painting dated to 1562 [34]. Such small smalt particles would likely further reduce the particles' tinting strength and as such a paint made with finely ground smalt may appear less blue [41]. The possibility that the smalt in the fragments is finely ground, then, may have consequences on the ability to detect smalt using reflectance spectroscopy.

Taken together, the lack of molecular evidence (i.e. color information) for smalt in these objects raises the intriguing question: why add smalt to ultramarine? The simplest answer may be to effectively adulterate costly ultramarine and increase profit for the pigment vendor. Alternatively, it is possible that a color vendor or artist was learning how to work with smalt early in its introduction to Europe, and either experimenting with particle size or unsure of the impacts of that size on overall color.

However, a more charitable and intriguing possibility comes from the observation that the Co-containing

ultramarine areas are used for less important parts of the scene in the manuscript fragments studied here. The areas of two fragments where ultramarine without cobalt was found (*Dormition of the Virgin* and *Saint Jerome*) relate to iconographically important components of the image such as the robes or attributes of the primary figures. Notably, among the six fragments, the same pigments are consistently used to create other colors that appear in the fragments (Table 2). Thus perhaps it is not surprising that the Master of the Murano Gradual may be using blue pigment mixtures selectively, and intentionally, in his work.

This selective use of ultramarine both with and without smalt (i.e. cobalt) is compelling and warrants further examination of other works by this artist, and contemporary artists working in and around Venice at this time

Table 2 Summary of the pigments found using non-invasive methods in the illuminated manuscript leaves

Color of areas	Dormition of the Virgin	St Blaise	St Jerome	St Lawrence	Initial G with The Nativity of the Virgin Mary	Camaldolese Saint
White	Lead white[b]	Lead white[a]	Lead white[a] Gypsum[b]	Lead white	Lead white Gypsum[b] (in mosaic gold)?	Lead white
Blue (inside main scene)	Ultramarine[b] Smalt (only in sky)[b] Lead white[b]	Ultramarine[a] Smalt Lead white[a,b]	Ultramarine[a] Lead white[a,b] Calcite[a]	ultramarine[b] Smalt Unknown blue[b]? (blue oval)	Ultramarine[a] Smalt Lead white[b]	n/a
Blue (outside/ surrounding decoration)	Ultramarine[b] Smalt[b] Lead white[b]	Ultramarine[a] Smalt Lead white[a,b] Calcite[a]	Ultramarine[a] Smalt Lead white[b]	ultramarine[b] Smalt Lead white[b]	Ultramarine[a] Smalt Lead white[b]	Ultramarine[a] Smalt Lead white[b]
Red	Red lead[b,c] Vermilion[b,c] Red earth Organic red[b,c]	Red lead (foliage)[a] Vermilion[a] Organic red?	Red lead (cardinal's hat)[a] Vermilion[a] Organic red?	Vermilion[b] (inner collar) Red lead[b] Organic red[b]? (pink marginalia)	Red Lead[a] Vermilion[a] Organic red[b] on calcium substrate?	Red lead (robe)[a] Organic red on calcium substrate?
Green	Copper green (likely verdigris)[b]	Copper green Carbon[a] Lead white[a]	Copper green Carbon[a]	Copper green	Copper green	Copper green
Flesh/ Hair	Lead white[b,c] Vermilion[b,c] Red earth[b,c] Mosaic gold (beard)[b,c] Carbon black (beard)[b,c]	Lead white[a] Vermilion[a] Iron oxide Mosaic gold (beard)[a] Lead tin yellow[a]	Lead white Vermilion[a] Iron oxide Carbon[a]	Lead white Vermilion Iron oxide Mosaic gold (hair) Shell gold (hair)	Lead white Vermilion[a] Iron oxide	Lead white Vermilion[a] Iron oxide Mosaic gold (beard)
Yellow	Mosaic gold[c] Lead tin yellow (type II?)[c]	Mosaic gold[a] Ochre Lead tin yellow[a]	Mosaic gold[a] Lead tin yellow[a]	Shell gold (design on robe) Lead tin yellow (highlights on green robe and leaves)	Lead tin yellow type I (robe)[a] Mosaic gold[a]	Mosaic gold[a] Lead tin yellow[a]
Black	Carbon black[c]	Carbon black[a] with copper-containing particles including azurite	Carbon black[a] with copper-containing particles	Carbon black[b]		
Metal	Gold leaf Silver		Gold leaf Shell gold	Gold leaf Silver	Gold leaf Shell gold (window grille)	Gold leaf
Bole	Vermilion	Vermilion[a] Lead white Iron oxide Gypsum?	Vermilion Lead white Iron oxide Gypsum?	Vermilion[b]	Vermilion[a] Lead white Iron oxide Gypsum?	Vermilion Lead white Iron oxide Gypsum?

Pigments inferred from XRF spectra (site-specific and scanning when available) unless additional techniques are noted

[a] Raman spectroscopy

[b] Fiber-optic reflectance spectroscopy

[c] Optical microscopy and near-infrared imaging

[18, 19]. Venice was the most important glassmaking centre of the 15th century, had long been a source of other pigments such as vermillion and lead white, and was the home of specialized shops, called "vendecolori", selling raw materials for painting, dyeing and glassmaking, about a century earlier than any other Italian city [42], thereby favouring reciprocal exchanges between artists and craftsmen [43]. In the context of material trade and the arts in Venice, then, additional research evaluating the production of cobalt-colored glasses in Italy, the relative chronology of smalt occurrences in illuminations, and the ways glass-based pigments are employed is necessary and ongoing.

Conclusions

The ability to correctly identify mixtures of smalt and ultramarine in the Master of the Murano Gradual's blue paints could have art historical implications. Therefore, we explored the various non-invasive tools available to conservation scientists that can identify smalt in the presence of ultramarine. Whereas invasive tools have mostly been used to identify smalt in 15th century paintings, such methods are often prohibited for illuminated manuscripts. The results of the testing here of four non-invasive methods that in mixtures with ultramarine, the mass concentration of smalt needs to be ~30–40% in order to be detected by reflectance spectroscopy, and even higher in order to be detectable by other molecular methods such as FTIR and Raman. The elemental method of XRF has high sensitivity (down to the ~1% level of smalt), through which the presence of smalt can be inferred due to the detection of cobalt. By looking for trace elements associated with the cobalt ore, and by doing high spatial resolution XRF area scans, one should be able to provide further evidence for the inference of smalt. The fragments studied here gave intriguing hints about iron possibly being associated with the cobalt ore, also supported by literature. No evidence for large, cobalt-rich particles were found by XRF linescans of the fragments, but overall the data does seem to point towards the presence of smalt, used selectively in some but not all blue passages, and perhaps not in a form or amount researchers are used to seeing in paintings. The example provided by the illuminations by the Master of the Murano Gradual, importantly, suggests that smalt as a minor phase in ultramarine rich areas may provide a marker for specific artist's practice, and influence our understanding of the introduction of new pigments in Venice more generally.

Supplementary Information

> **Additional file 1: Fig. S1.** Visible light images of the mock-up samples. (a) Mixtures of synthetic ultramarine and smalt in gum Arabic (Set 1); (b) mixtures of synthetic ultramarine, smalt, and titanium white in acrylic (Set 2).
>
> **Additional file 2: Fig. S2.** Area ratios calculated for XRF spectra of Set 1 paint-outs (XRF parameters: 15 kV, 1200 µA, He flush).
>
> **Additional file 3: Table S1.** Summary of samples and illuminated manuscript fragments analyzed, all attributed to the Master of the Murano Gradual. Abbreviations used: NGA = National Gallery of Art, Washington DC; FM = Fitzwilliam Museum; JPGM = J. Paul Getty Museum; GCI = Getty Conservation Institute

Authors' contributions
PR initiated and planned this research. PR and JKD designed the experiments and samples with assistance from FG and GB. All authors collected and interpreted data. PR, GB, CSP, and DM wrote the first draft of the manuscript. KD, JKD, CSP, PR, and DM wrote and edited the subsequent versions of the manuscript. All authors read and approved the final manuscript.

Availability of data and materials
The data is available from the authors upon request and pending permission from the institutions that house the art objects.

Declarations

Competing interests
The authors declare that they have no competing interests.

Author details
[1]The Fitzwilliam Museum, University of Cambridge, Trumpington Street, Cambridge CB2 1RB, UK. [2]National Gallery of Art, 6th Street and Constitution Avenue NW, Washington, DC 20565, USA. [3]Getty Conservation Institute, 1200 Getty Center Drive, Los Angeles, CA 90049, USA. [4]Present Address: School of Clinical Medicine, University of Cambridge, Addenbrooke's Hospital, Hills Rd, Cambridge CB2 0SP, UK. [5]Present Address: Scientific Department, Rijksmuseum, Museumstraat 1 1071 DN, Amsterdam, Netherlands.

Ricciardi *et al. Heritage Science*   (2022) 10:38

Page 17 of 18

References

1. Oltrogge D. "Pro lazurio auricalco et alii correquisitis pro illuminacione": The Werden accounts and other sources on the trade in manuscript materials in the Lower Rhineland and Westphalia around 1500. In: Kirby J, Nash S, Cannon J, editors. Trade in artists' materials: markets and commerce in Europe to 1700. London: Archetype Publications; 2010. p. 189–98.
2. Spufford P. Lapis, Indigo, Woad: artists' materials in the context of international trade before 1700. In: Kirby J, Nash S, Cannon J, editors. Trade in artists' materials: markets and commerce in Europe to 1700, vol. 1700. London: Archetype Publications; 2010. p. 10–28.
3. Bucklow S. The trade in colours. In: Panayotova S, Jackson D, Ricciardi P, editors. Colour: the art and science of illuminated manuscripts. London and Turnhout: Harvey Miller Publishers; 2016. p. 59–65.
4. Spear RE. A century of pigment prices: seventeenth-century Italy. In: Kirby J, Nash S, Cannon J, editors. Trade in artists' materials: markets and commerce in Europe to 1700, vol. 1700. London: Archetype Publications; 2010. p. 275–96.
5. Berrie BH. Mining for color: new blues, yellows, and translucent paint. Early Sci Med. 2015;20(4–6):308–34. https://doi.org/10.1163/15733823-02046p02.
6. Dunkerton J, Spring M, Billinge R, Howard H, et al. Titian after 1540 technique and style in his later works. Natl Gall Tech Bull. 2015;36:6–39.
7. Mahon D, Centeno SA, Wypyski MT, Salomon XF, et al. Technical study of three allegorical paintings by Paolo Veronese: "The Choice between Virtue and Vice," "Wisdom and Strength," and "Mars and Venus United by Love." Metrop Mus Stud Art Sci Technol. 2010;1:83–108.
8. Poldi G. Gli azzurri perduti nei dipinti di Tintoretto. Ri-vedere le cromie grazie alle analisi scientifiche. La Crocifissione di Tintoretto. L'intervento sul dipinto dei Musei civici di Padova. S. Abram. Torino, La Crocifissione di Tintoretto. L'intervento sul dipinto dei Musei Civici di Padova, Editris; 2013. 2000: 101–14.
9. Lutzenberger K, Stege H, Tilenschi C. A note on glass and silica in oil paintings from the 15th to the 17th century. J Cult Herit. 2010;11(4):365–72. https://doi.org/10.1016/j.culher.2010.04.003.
10. Spring M. Colourless powdered glass as an additive in fifteenth- and sixteenth-century European Paintings. Natl Gall Tech Bull. 2012;33:4–26.
11. Cavallo G, Riccardi MP. Glass-based pigments in painting: smalt blue and lead–tin yellow type II. Archaeol Anthropol Sci. 2021. https://doi.org/10.1007/s12520-021-01453-7.
12. Mühlethaler B, Thissen J. Smalt. In: Roy A, editor. Artists' pigments: a handbook of their history and characteristics, vol. 2. Washington: National Gallery of Art; 1993. p. 113–30.
13. Turner NK, Schmidt Patterson C. New discoveries in the painting materials in the Medieval Mediterranean: connections between manuscript illumination and glass technology during the Byzantine Era, c.1100–1300. In: Panayotova S, Ricciardi P, editors. Manuscripts in the making: art and science, vol. 1. London, Turnhout: Harvey Miller Publishers; 2017. p. 185–97.
14. Bomford D, Roy A, Smith A. The techniques of Dieric Bouts: two paintings contrasted. Natl Gall Tech Bull. 1986;10:39–57.
15. Stege H. Out of the Blue? Considerations on the early use of smalt as blue pigment in European easel painting. Kunsttechnologie Konservierung. 2004;18(1):121–42.
16. Panayotova S, Turner N. Cat. 81: Fitzwilliam Museum, Marlay cutting it. In: Panayotova S, Jackson D, Ricciardi P, editors. 18 Colour: the art and science of illuminated manuscripts. London and Turnhout: Harvey Miller Publishers; 2016. p. 287–8.
17. Panayotova S, Ricciardi P, Turner N. Master of the Murano Gradual (act. c.1420–1450). In: Panayotova S, editor. The art and science of illuminated manuscripts. A handbook. London/Turnhout: Harvey Miller/Brepols; 2020. p. 378–84.
18. Ricciardi P, Mazzinghi A, Legnaioli S, Ruberto C, et al. The choir books of San Giorgio Maggiore in Venice: results of in depth non-invasive analyses. Heritage. 2019;2(2):1684–701. https://doi.org/10.3390/heritage2020103.
19. Ricciardi P, Mazzinghi A, Panayotova S. I corali di San Giorgio Maggiore. Le analisi scientifiche (The choir books of San Giorgio Maggiore. Scientific analyses). In: C. Ponchia and F. Toniolo, editors. I Corali miniati di San Giorgio Maggiore a Venezia. L'inCanto della miniatura. Cinisello Balsamo. 2020.
20. Aceto M, Agostino A, Fenoglio G, Gulmini M, et al. Non invasive analysis of miniature paintings: proposal for an analytical protocol. Spectrochim Acta Part A Mol Biomol Spectrosc. 2012;91:352–9. https://doi.org/10.1016/j.saa.2012.02.021.
21. Delaney JK, Riccardi P, Glinsman LD, Facini M, et al. Use of imaging spectroscopy, fiber optic reflectance spectroscopy, and X-ray fluorescence to map and identify pigments in illuminated manuscripts. Stud Conserv. 2014;59(2):91–101. https://doi.org/10.1179/2047058412y.0000000078.
22. Ricciardi P, Schmidt Patterson C. Science of the book: analytical methods for the study of illuminated manuscripts. In: Panayotova S, editor. The art and science of illuminated manuscripts: a handbook. London: Harvey Miller/Brepols; 2020. p. 51–87.
23. Freuler G. 78. Master of San Michele A Murano, Venice, c. 1420–25. In: Freuler G, Kidd P, Parpulov G, McCarthy R, editors. Initial G with the nativity of the Virgin Mary, from a Gradual. The McCarthy Collection, vol. I. London: Ad Ilissum; 2018. p. 244–6.
24. Panayotova S. Master of the Murano Gradual. In: Hindman S, Toniolo F, editors. The Burke collection of Italian manuscript paintings. London: AD ILISSVM (an imprint of Paul Holberton Publishing); 2021. p. 389–97.
25. Conover DM. Fusion of reflectance and X-ray fluorescence imaging spectroscopy data for the improved identification of artists' materials, The George Washington University, Ph.D. thesis. 2015.
26. Alfeld M, Janssens K. Strategies for processing mega-pixel X-ray fluorescence hyperspectral data: a case study on a version of Caravaggio's painting Supper at Emmaus. J Anal Atom Spectrom. 2015;30(3):777–89. https://doi.org/10.1039/c4ja00387j.
27. Solé VA, Papillon E, Cotte M, Walter P, et al. A multiplatform code for the analysis of energy-dispersive X-ray fluorescence spectra. Spectrochim Acta Part B Atom Spectrosc. 2007;62(1):63–8. https://doi.org/10.1016/j.sab.2006.12.002.
28. Wolff T, Malzer W, Mantouvalou I, Hahn O, et al. A new fundamental parameter based calibration procedure for micro X-ray fluorescence spectrometers. Spectrochim Acta Part B Atom Spectrosc. 2011;66(2):170–8. https://doi.org/10.1016/j.sab.2011.01.009.
29. Bacci M, Picollo M. Non-destructive spectroscopic detection of cobalt(II) in paintings and glass. Stud Conserv. 1996;41(3):136–44. https://doi.org/10.1179/sic.1996.41.3.136.
30. Aceto M, Agostino A, Fenoglio G, Idone A, et al. Characterisation of colourants on illuminated manuscripts by portable fibre optic UV-visible-NIR reflectance spectrophotometry. Anal Methods. 2014;6(5):1488. https://doi.org/10.1039/c3ay41904e.
31. Vetter W, Schreiner M. Characterization of pigment-binding media systems—comparison of non-invasive in-situ reflection FTIR with transmission FTIR microscopy. e-Preserv Sci. 2011;8:10–22.
32. Miliani C, Rosi F, Daveri A, Brunetti BG. Reflection infrared spectroscopy for the non-invasive in situ study of artists' pigments. Appl Phys A. 2012;106(2):295–307. https://doi.org/10.1007/s00339-011-6708-2.
33. Nodari L, Ricciardi P. Non-invasive identification of paint binders in illuminated manuscripts by ER-FTIR spectroscopy: a systematic study of the influence of different pigments on the binders' characteristic spectral features. Herit Sci. 2019;7:7. https://doi.org/10.1186/s40494-019-0249-y.
34. Spring M, Higgitt C, Saunders D. Investigation of pigment-medium interaction processes in oil paint containing degraded smalt. Natl Gall Tech Bull. 2005;26:56–70.
35. . "Infrared and Raman User's Group." from http://www.irug.org/search-spectral-database?spectra_front_form_filter%5Bkeyword%5D%5Btext%5D=smalt&spectra_front_form_filter%5Bdata_type%5D=&spectra_front_form_filter%5Bmaterial_class%5D=.
36. Clark RJH. Raman microscopy: application to the identification of pigments on medieval manuscripts. Chem Soc Rev. 1995;24(3):187–98.
37. Burgio L. Analysis of pigments on manuscripts by Raman spectroscopy: advantages and limitations. In: Neate S, Howell D, Ovenden R, Pollard AM, editors. The technological study of books and manuscripts as artefacts: research questions and analytical solutions. Oxford: Archaeopress; 2011.
38. Clark RJH, Franks ML. The resonance raman spectrum of ultramarine blue. Chem Phys Lett. 1975;34(1):69–72.

39. Krishnamurti D. The Raman spectrum of quartz and its interpretation. Proc Indian Acad Sci Sect A. 1958. https://doi.org/10.1007/BF03052811.

40. Bell IM, Clark RJH, Gibbs PJ. Raman spectroscopic library of natural and synthetic pigments (pre- ~1850 AD). Spectrochim Acta Part a Mol Biomol Spectrosc. 1997;53(12):2159–79.

41. van Loon A, Noble P, de Man D, Alfeld M, et al. The role of smalt in complex pigment mixtures in Rembrandt's Homer 1663: combining MA-XRF imaging, microanalysis, paint reconstructions and OCT. Herit Sci. 2020;8:90. https://doi.org/10.1186/s40494-020-00429-5.

42. Berrie BH, Matthew LC. Material Innovation and Artistic Invention: New Materials and New Colors in Renaissance Venetian Paintings. Scientific Examination of Art: Modern Techniques in Conservation and Analysis. Washington, D.C., The National Academies Press; 2005. pp 12–26.

43. Matthew LC. "Vendecolori a Venezia": the reconstruction of a profession. Burlington Mag. 2002;144(1196):680–6.

Publisher's Note